Supplementary Information for

A Computational Framework for Modeling & Simulating Vibrational Mode Dynamics

The following topics are discussed in this supplementary information:

Supercell lattice dynamics.

ModeCode program.

Phonon dynamics simulations.

Relation of mode coupling constants to phonon scattering rates.

Finite-temperature wave-packet simulations.

Interfacial heat transfer in mode coordinates.

Supercell lattice dynamics.

Supercell lattice dynamics is the procedure of finding the vibrational modes (frequencies and eigenvectors) for supercell of atoms, which may contain many unit cells in a crystalline solid, or a large structure without perfect crystal symmetry (e.g. amorphous material, alloy, interface, etc.). The frequencies and eigenvectors of normal modes for a solid in a supercell are defined by the harmonic part of the atomic equations of motion, $m_i \ddot{u}_i^\alpha = -\sum_{j,\beta} \Phi_{ij}^{\alpha\beta} u_j^\beta$. The exact solution of this 2nd order differential equation is a well-known in lattice dynamics[1] and takes the form of an eigenvalue problem. Usually this eigenvalue problem is solved for all wave-vectors in a periodic crystal to obtain phonon dispersion curves[2], but here we are interested in modes arising

in non-crystalline systems, so we solve the eigenvalue problem at the gamma point (zero wave-vector) in a large supercell of atoms. After substituting general solutions $u_i^{\alpha}(t) = \frac{1}{\sqrt{m_i}} \sum_n X_n e_{ni}^{\alpha} e^{-i\omega_n t}$, where $e^{-i\omega_n t}$ is a time exponential showing the oscillatory behavior of a single mode, the harmonic equation of motion $m_i \ddot{u}_i^{\alpha} = -\sum_{j,\beta} \Phi_{ij}^{\alpha\beta} u_j^{\beta}$ can be written in the form of the eigenvalue equation[1]

$$\mathbf{e} \cdot \mathbf{\Omega} = \mathbf{D} \cdot \mathbf{e} \tag{1}$$

where $\mathbf{e}$ are matrices of eigenvectors, with each column representing the eigenvector of a single mode, organized like[1]

$$\begin{matrix} e_{11}^{x} & e_{21}^{x} & e_{31}^{x} & \cdots & e_{3N,1}^{x} \\ e_{11}^{y} & e_{21}^{y} & e_{31}^{y} & \cdots & e_{3N,1}^{y} \\ e_{11}^{z} & e_{21}^{z} & e_{31}^{z} & \cdots & e_{3N,1}^{z} \\ e_{12}^{x} & e_{22}^{x} & e_{32}^{x} & \cdots & e_{3N,2}^{x} \\ e_{12}^{y} & e_{22}^{y} & e_{32}^{y} & \cdots & e_{3N,2}^{y} \\ \vdots & \vdots & \vdots & \ddots & \vdots \\ e_{1N}^{z} & e_{2N}^{z} & e_{2N}^{z} & \cdots & e_{3N,N}^{y} \end{matrix} \tag{2}$$

where the eigenvector components e_{ni}^{α} are indexed by mode n, atom i, Cartesian direction α, and the mode indices run from 1 to $3N$ (N being the number of atoms). The $\mathbf{\Omega}$ in Equation 1 is a diagonal matrix of eigenvalues which are the squared frequencies of modes given by

$$\begin{matrix} \omega_1^2 & 0 & 0 & 0 \\ 0 & \omega_2^2 & 0 & 0 \\ 0 & 0 & \ddots & 0 \\ 0 & 0 & 0 & \omega_{3N}^2 \end{matrix} \tag{3}$$

where ω_n is the frequency of mode n. The dynamical matrix $\mathbf{D}$ is an $N \times N$ array of smaller 3×3 matrices; the elements of these 3×3 blocks are given by

$$D_{ij}^{\alpha\beta} = \frac{\Phi_{ij}^{\alpha\beta}}{\sqrt{m_i m_j}} \tag{4}$$

where the position of this element in the full dynamical matrix $\mathbf{D}$ is given by row $3(i-1)+\alpha$ and column $3(j-1)+\beta$.[1] We made the open-source program ModeCode[3] to aid in calculating this dynamical matrix and solving the eigenvalue problem of Equation 1 to get the mode frequencies and eigenvectors for large supercells of atoms. In our open-source code, we also provide LAMMPS files to aid in the calculation of mode amplitudes and velocities at each timestep in a MD simulation. We note here that obtaining the mode amplitudes and velocities at every timestep in a MD simulation brings an additional cost which involves a double loop over all atoms: one loop over all modes (3 times the number of atoms), and another loop over all atoms and Cartesian directions, to calculate the mode amplitudes and velocities $X_n = \sum_{i,\alpha} \sqrt{m_i} u_i^{\alpha} e_{ni}^{\alpha}$ and $\dot{X}_n = \sum_{i,\alpha} \sqrt{m_i} \dot{u}_i^{\alpha} e_{ni}^{\alpha}$, respectively.

One can understand the meaning of mode amplitude and velocity by considering the following illustration.

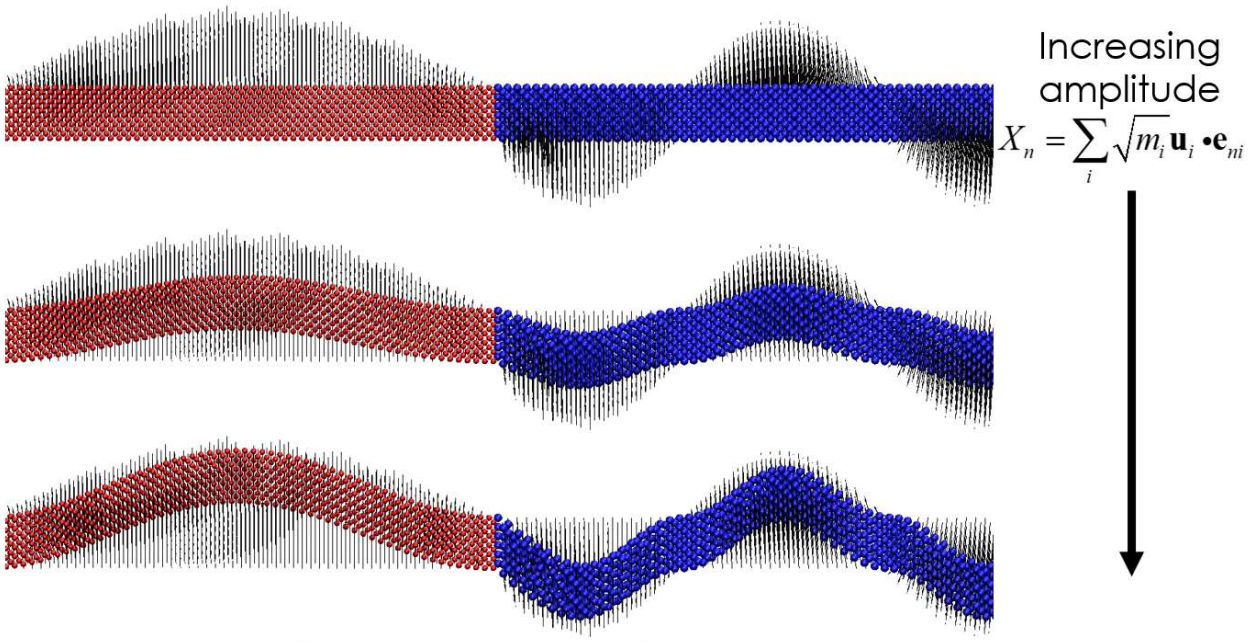

Figure 1. A mode in the same 4320 atom silicon-germanium superlattice system that we studied in the manuscript. Red atoms are silicon and blue are germanium. The eigenvectors are plotted as black arrows on the atoms. This illustration shows that the mode amplitude $X_n = \sum_i \sqrt{m_i}\mathbf{u}_i \bullet \mathbf{e}_{ni}$ *is a quantity that increases as the atoms are displaced along the eigenvectors of a mode. Likewise, the mode velocity* $\dot{X}_n = \sum_i \sqrt{m_i}\mathbf{v}_i \bullet \mathbf{e}_{ni}$ *is the time-rate of change of this mode amplitude, or a measure of how fast the atoms are vibrating along the mode eigenvectors.*

The mode velocity is not to be confused with the phonon group velocity, because the modes we extract are standing wave solutions to the equations of motion written as an eigenvalue problem in Equation 1, meaning that individual modes do not propagate energy like a traveling wave would. The phonon group velocity is the velocity of the disturbance created by combining multiple modes, as in the commonly used wave-packet method in MD simulations. The mode force defined in our manuscript, on the other hand, is conceptually the acceleration of a mode, or how fast the mode

velocity is changing with time. The mode equations of motion we derived relate this acceleration to the amplitude of other modes via $\frac{d\dot{X}_n}{dt} = -\omega_n^2 X_n - \frac{1}{2}\sum_{nml} K_{nml} X_m X_l - \cdots$, so the inter-mode forces are the anharmonic terms $K_{nml} X_m X_l$ which determine how the amplitudes of two modes m and l influences the acceleration or "force" of a mode n. Conceptually, these inter-mode forces arise because when two modes m and l have a finite amplitude, the atoms in these modes exert anharmonic forces on the atoms in mode n, so the inter-mode force is an effective anharmonic interatomic force exerted on atoms between modes.

ModeCode program.

Once the eigenvectors for all modes in the system are calculated via Equation 1, quantities that depend on the eigenvectors such as mode coupling constants, mode participation ratios, and others, are readily calculated with our ModeCode program. ModeCode is a massively parallel and modular program that aids in the study of vibrational modes. Vibrational modes are collective movements in a system, which vibrate at certain frequencies. In atomic systems, these collective motions are composed of atoms which vibrate at specific frequencies. All the motion in an atomic system is determined by Newton's 2nd law, and this motion may be decomposed into the individual modes. These motions influence all phenomena that we observe in materials, including thermal and electrical transport, mass diffusion, and chemical reactions. It is of therefore great interest to develop a program that aids in the general study of vibrational modes for systems with arbitrary size, geometry, and composition, which spans a great variety of systems studied by the molecular dynamics community. ModeCode is the first program is the first of its kind, as all other open-source programs only deal with vibrational modes/phonons in ideal crystals. By interfacing with a large library of interatomic potentials (LAMMPS[4]) and alleviating the assumption of periodicity,

ModeCode allows for the study of vibrational modes in all materials. The software structure of the program is shown in Figure 2 below.

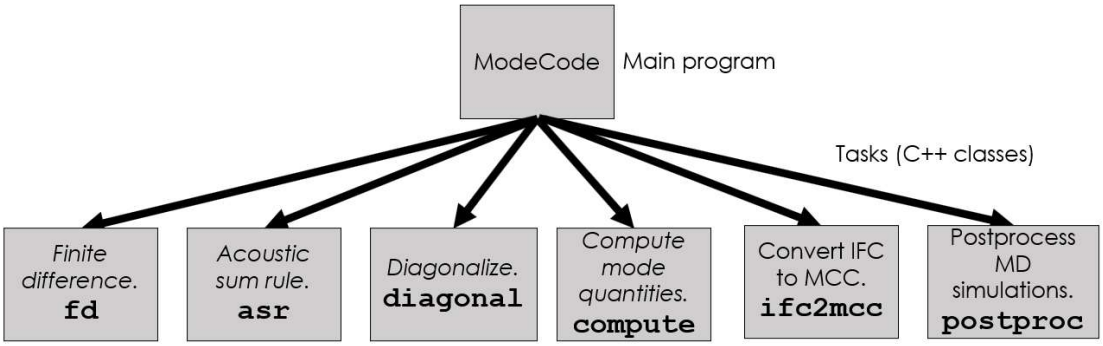

Figure 2. ModeCode high-level software structure, showing the main tasks (each a separate class in C++) of the program.

The "fd" task performs finite difference to calculate the IFCs, using any potential in the LAMMPS library of potentials. The "asr" task performs acoustic sum rule calculations on the IFCs. The "diagonal" task diagonalizes the dynamical matrix to get the frequencies and eigenvectors of modes. The "compute" task calculates mode quantities that depend on the eigenvectors, such as participation ratio. The "ifc2mcc" task converts IFCs to mode coupling constants. Finally, the "postproc" class postprocesses MD simulation data to calculate quantities such as autocorrelations of heat flux due to pairs of modes to get thermal conductivity. These tasks and updates/upgrades are maintained online at https://github.com/rohskopf.

Phonon dynamics simulations.

One utility of ModeCode is to aid in the phonon dynamics simulations, where energy transfer between modes is simulated within MD simulations, and there are multiple ways of achieving this.

There are three equivalent methods for simulating phonon dynamics, which we explain here. In our manuscript we used Method 2.

Method 1: Perform simulations in mode space, using velocity Verlet integration with mode coordinates. This is illustrated below.

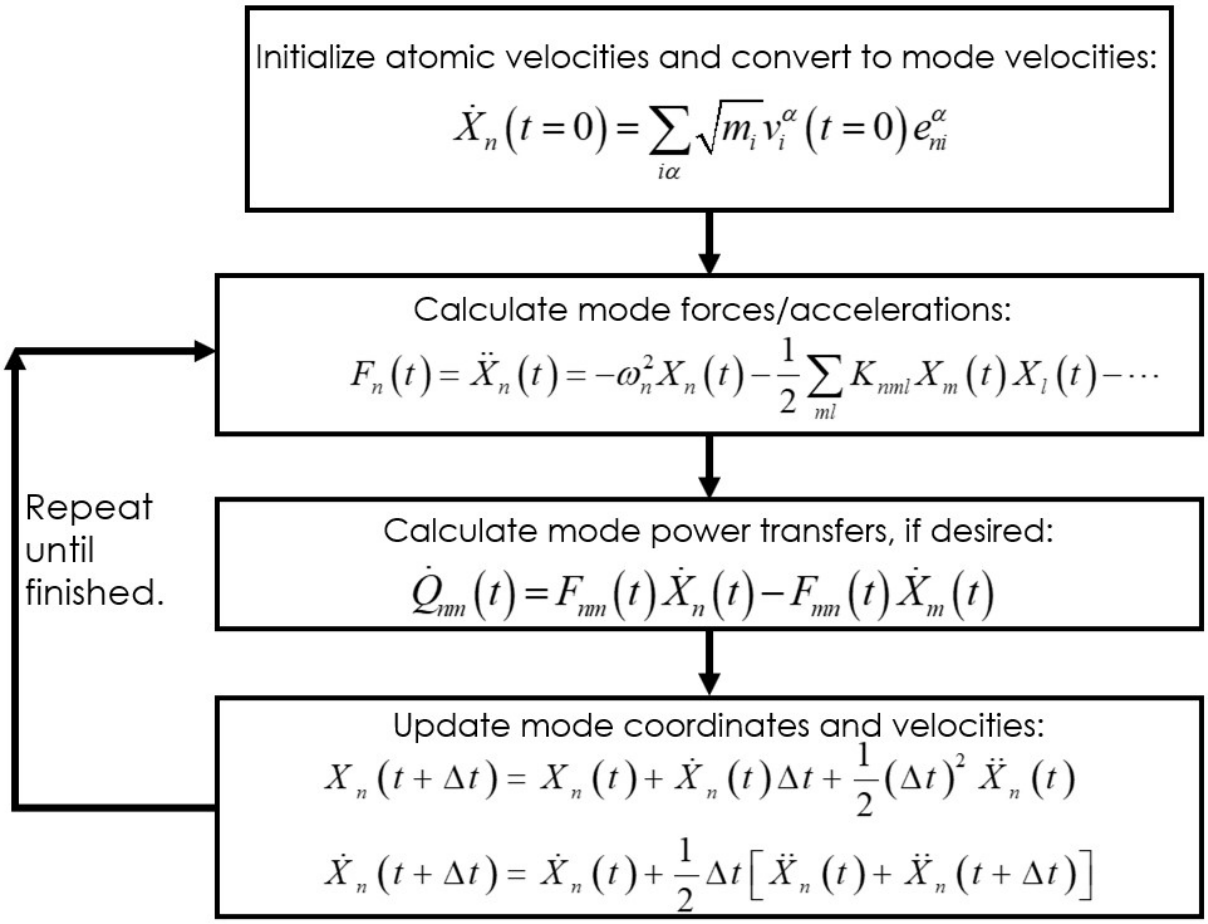

Figure 3. Method 1 of simulating phonon dynamics involve first performing MD simulations and saving the atomic coordinates, and then postprocessing to calculate mode coordinates and mode forces as a function of time.

Method 2: Perform simulations in real space using MD, and calculate the mode coordinates, forces, and power transfer at desired timesteps, during the simulation. This is illustrated below.

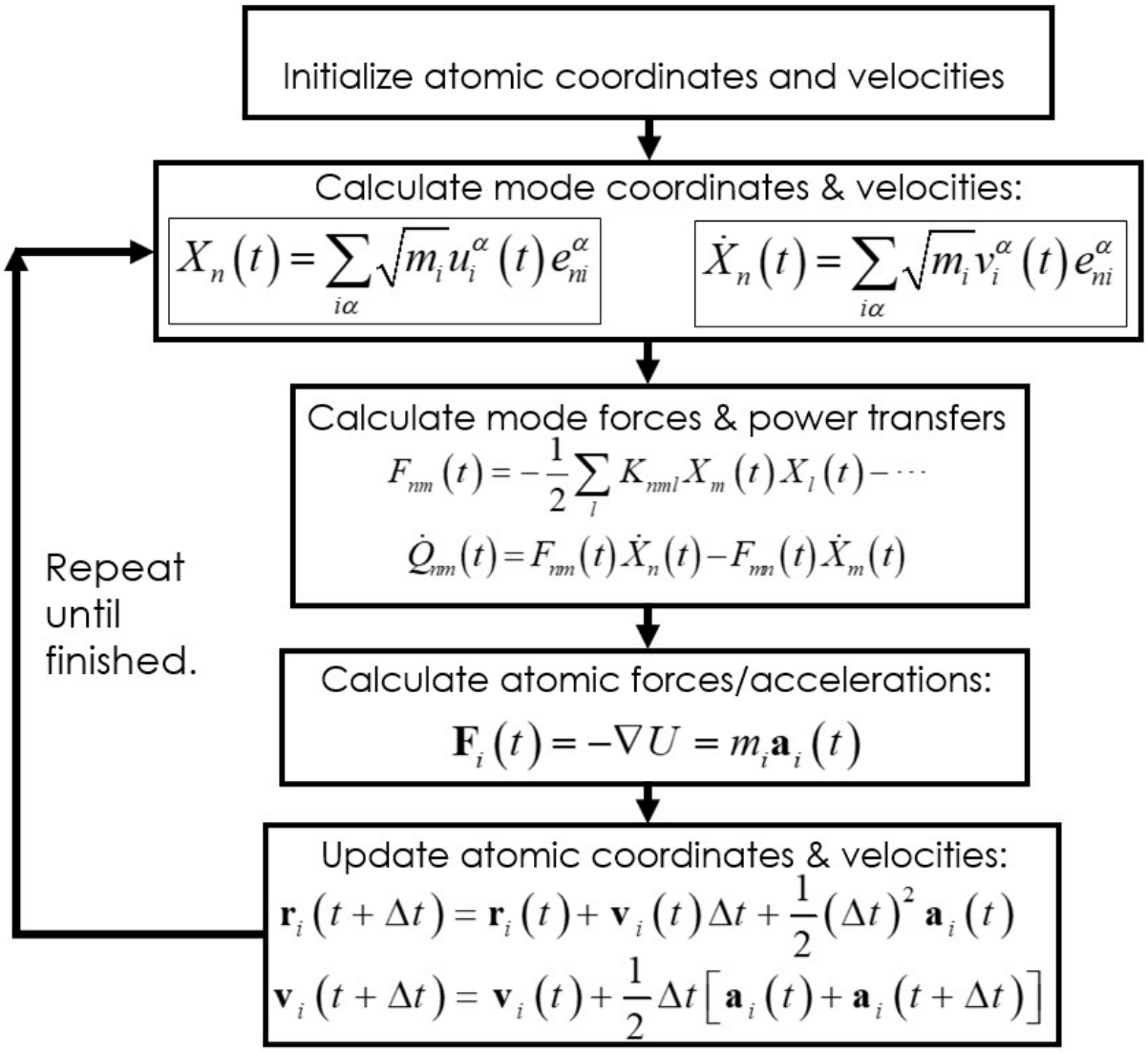

Figure 4. Method 2 of simulating phonon dynamics involves postprocessing the atomic trajectories from MD at each timestep, requiring the ModeCode custom compute classes in LAMMPS. This is the method used in our manuscript.

Method 3: Perform simulations in real space using MD, and then postprocess the atomic trajectories to calculate mode coordinates, forces, and power transfer at desired timesteps.

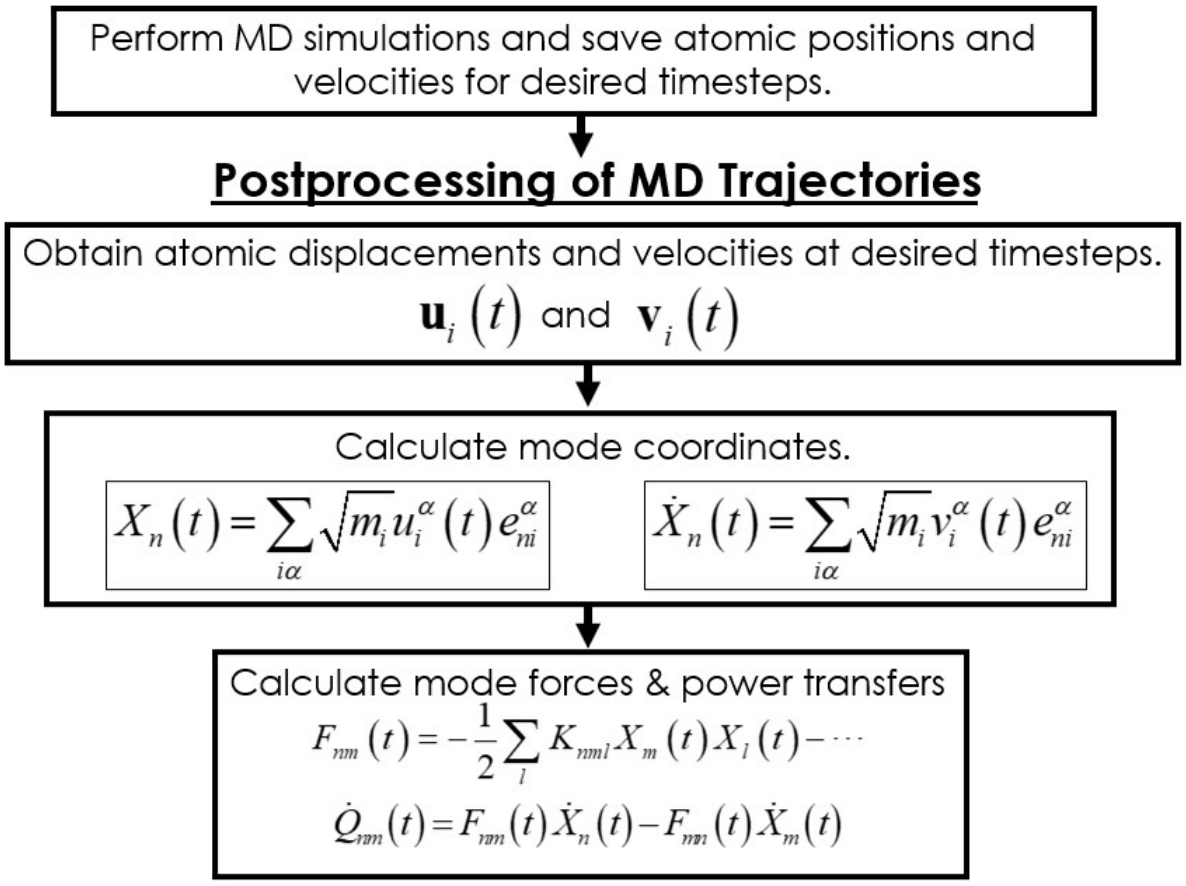

Figure 5. Method 3 of simulating phonon dynamics involve first performing MD simulations and saving the atomic coordinates, and then postprocessing to calculate mode coordinates and mode forces as a function of time.

MD is therefore a tool for simulating phonon interactions. ModeCode allows one to calculate the eigenvectors and coupling constants for performing these calculations, and then perform the postprocessing to calculate inter-mode forces and inter-mode energy transfer either during or after MD simulations. ModeCode couples to LAMMPS to calculate the coupling

constants and has custom LAMMPS computes to perform the mode force calculations via Method 2 in Figure 4 during a MD simulation. We note that one could also perform velocity Verlet integration in mode space via Method 1, but this is not as practical because one would then need to store the coupling constants for all mode interactions in the system, when only a few mode interactions may be of interest. Regardless, ModeCode also offers the option for performing simulations in mode space as well.

When calculating the inter-mode forces, one must store a matrix of 3rd order coupling constants (MCC3s) $K_{nml} = \sum_{ijk} \sum_{\alpha\beta\gamma} \frac{\Psi_{ijk}^{\alpha\beta\gamma} e_{ni}^{\alpha} e_{mj}^{\beta} e_{lk}^{\gamma}}{\sqrt{m_i m_j m_k}}$. These are calculated via ModeCode and stored before the simulation if using Methods 1 or 2, or calculated before postprocessing MD trajectories via Method 3. One may not need to store the vast number of MCC3s because only a small percent often comprise the top few orders of magnitude, as shown in Figure 6 below.

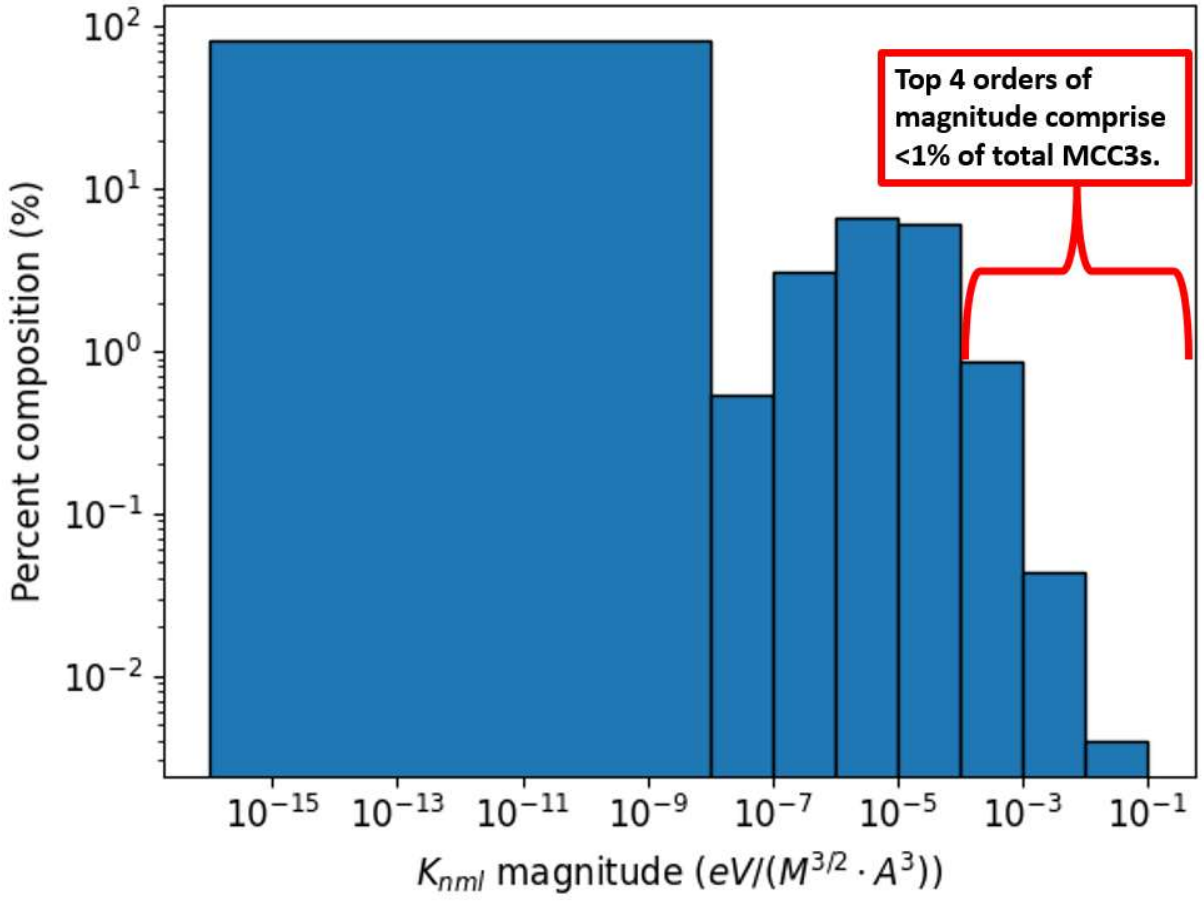

Figure 6. Figure 7. Average MCC3 distribution for the longitudinal wave-packet modes in our study. The MCC3s are binned by magnitude with units of eV/($M^{3/2}$Å^{3}) where M is molar mass (g/mol). As shown in the figure, the top ~3-4 orders of magnitude comprise < 1% of the total MCC3s.

Relation of mode coupling constants to phonon scattering rates.

The phonon linewidth $\Gamma_{n}\left(\mathbf{q},\omega\right)$ (inverse of relaxation time) for mode n with wave-vector $\mathbf{q}$ is given by[5]

$$\begin{aligned}\Gamma_n(\mathbf{q},\omega) = \frac{\pi}{2\hbar^2}\sum_{\mathbf{q}_1,\mathbf{q}_2}\sum_{ml}\left|V^{(3)}_{-\mathbf{q}n,\mathbf{q}_1 m,\mathbf{q}_2 l}\right|^2 \\ \times\Big[\left(f_1+f_2+1\right)\delta\left(\omega_n-\omega_1-\omega_2\right) \\ -\left(f_1+f_2+1\right)\delta\left(\omega_n+\omega_1+\omega_2\right) \\ +(f_1-f_2)\delta\left(\omega_n+\omega_1-\omega_2\right) \\ -(f_1-f_2)\delta\left(\omega_n-\omega_1+\omega_2\right)\Big]\end{aligned} \tag{5}$$

where $\mathbf{q}_i$ are phonon wave-vectors, nml are mode indices, and f is the Bose-Einstein distribution function. The terms $V^{(3)}_{-\mathbf{q}n,\mathbf{q}_1 m,\mathbf{q}_2 l}$ are the coefficient of three-phonon interactions, defined by[5,6]

$$\begin{aligned}V^{(3)}_{-\mathbf{q}n,\mathbf{q}_1 m,\mathbf{q}_2 l} = \left(\frac{\hbar}{2N_q}\right)^{3/2}\frac{1}{\sqrt{\omega_n(\mathbf{q})\omega_m(\mathbf{q}_1)\omega_l(\mathbf{q}_2)}} \\ \times\sum_{\mathbf{n}_1,\mathbf{n}_2,\mathbf{n}_3}\exp\left[i\left(\mathbf{q}\bullet\mathbf{n}_1+\mathbf{q}_1\bullet\mathbf{n}_2+\mathbf{q}_2\bullet\mathbf{n}_3\right)\right] \\ \times\sum_{a_1,a_2,a_3}\sum_{\alpha\beta\gamma}\Psi^{\alpha\beta\gamma}_{a_1\mathbf{n}_1,a_2\mathbf{n}_2,a_3\mathbf{n}_3} \\ \times\frac{e^{\alpha}_{ni}(\mathbf{q})e^{\beta}_{mj}(\mathbf{q}_1)e^{\gamma}_{lk}(\mathbf{q}_2)}{\sqrt{m_i m_j m_k}}\end{aligned} \tag{6}$$

where N_q is the number of periodic primitive cells. In our manuscript, we performed supercell lattice dynamics calculations where we only consider gamma point modes, so we perform all lattice dynamics calculations at the gamma point, i.e. $\mathbf{q}=\mathbf{q}_1=\mathbf{q}_2=0$. The coefficient of three-phonon interactions then reduces to

$$V^{(3)}_{nml} = \left(\frac{\hbar}{2}\right)^{3/2}\frac{K_{nml}}{\sqrt{\omega_n\omega_m\omega_l}} \tag{7}$$

where K_{nml} are the mode coupling constants (MCC3s) defined in our manuscript. At the gamma point, the 2nd order perturbation theory expression for phonon scattering rate therefore becomes

$$\begin{aligned}\Gamma_n = & \frac{\hbar\pi}{16\omega_n}\sum_{\mathbf{q}_1,\mathbf{q}_2}\sum_{ml}\left|\frac{K_{nml}}{\omega_m\omega_l}\right|^2 \\ & \times\Big[\left(f_1+f_2+1\right)\delta\left(\omega_n-\omega_1-\omega_2\right) \\ & -\left(f_1+f_2+1\right)\delta\left(\omega_n+\omega_1+\omega_2\right) \\ & +\left(f_1-f_2\right)\delta\left(\omega_n+\omega_1-\omega_2\right) \\ & -\left(f_1-f_2\right)\delta\left(\omega_n-\omega_1+\omega_2\right)\Big]\end{aligned} \tag{8}$$

which is the gamma point $\mathbf{q}=0$ form of Equation 5. These derivations show that our mode coupling constants are the same ones used in the traditional concept of 3-phonon interactions, except we perform calculations for a large supercell of atoms at the gamma point.

Finite-temperature wave-packet simulations.

The finite-temperature wave-packet method involves initializing a phonon wave-packet in a finite-temperature environment, so that many anharmonic energy transfer pathways are activated. To achieve this, we initialize modes associated with LA phonon wave-packets using the atomic displacements[7,8]

$$u_i^{\alpha} = Ae_i^{\alpha}\left(k_0\right)\exp\left[ik_0\left(z_i-z_0\right)\right]\exp\left[-\frac{\left(z_i-z_0\right)^2}{\xi^2}\right] \tag{9}$$

where A is an amplitude representing the magnitude of displacement, $e_i^{\alpha}\left(k_0\right)$ is the polarization vector of mode eigenvector components, k_0 is the reduced wave-vector, z_i is the Cartesian z

coordinate of atom i with z_0 as the initial wave-packet position in real-space, and ξ is the spatial extent of the wave-packet. It is important to note that Equation 9 along with its time derivative (atomic velocity v_i^α) constitute a wave-packet which gives a unique signature of mode amplitude and velocity through the Fourier series representations $X_n = \sum_{i,\alpha} \sqrt{m_i} u_i^\alpha e_{ni}^\alpha$ and $\dot{X}_n = \sum_{i,\alpha} \sqrt{m_i} v_i^\alpha e_{ni}^\alpha$. Using these unique combinations of mode amplitude and velocity which constitute a wave-packet, we force a wave-packet to exist in a finite temperature environment by first initializing the system with randomized velocities, and then recalculating positions and velocities so that $u_i^\alpha = \frac{1}{\sqrt{m_i}} \sum_n X_n e_{ni}^\alpha$ and $v_i^\alpha = \frac{1}{\sqrt{m_i}} \sum_n \dot{X}_n e_{ni}^\alpha$, where X_n and $\dot{X}_n$ are the mode amplitudes and velocities associated with the wave-packet. For all wave-packet simulations, we use a 4320-atom Si-Ge superlattice modelled by a neural network potential that was trained against *ab initio* forces and shown to accurately reproduce interfacial thermal transport[9]. MD simulations were performed using LAMMPS[4]. This procedure is illustrated below.

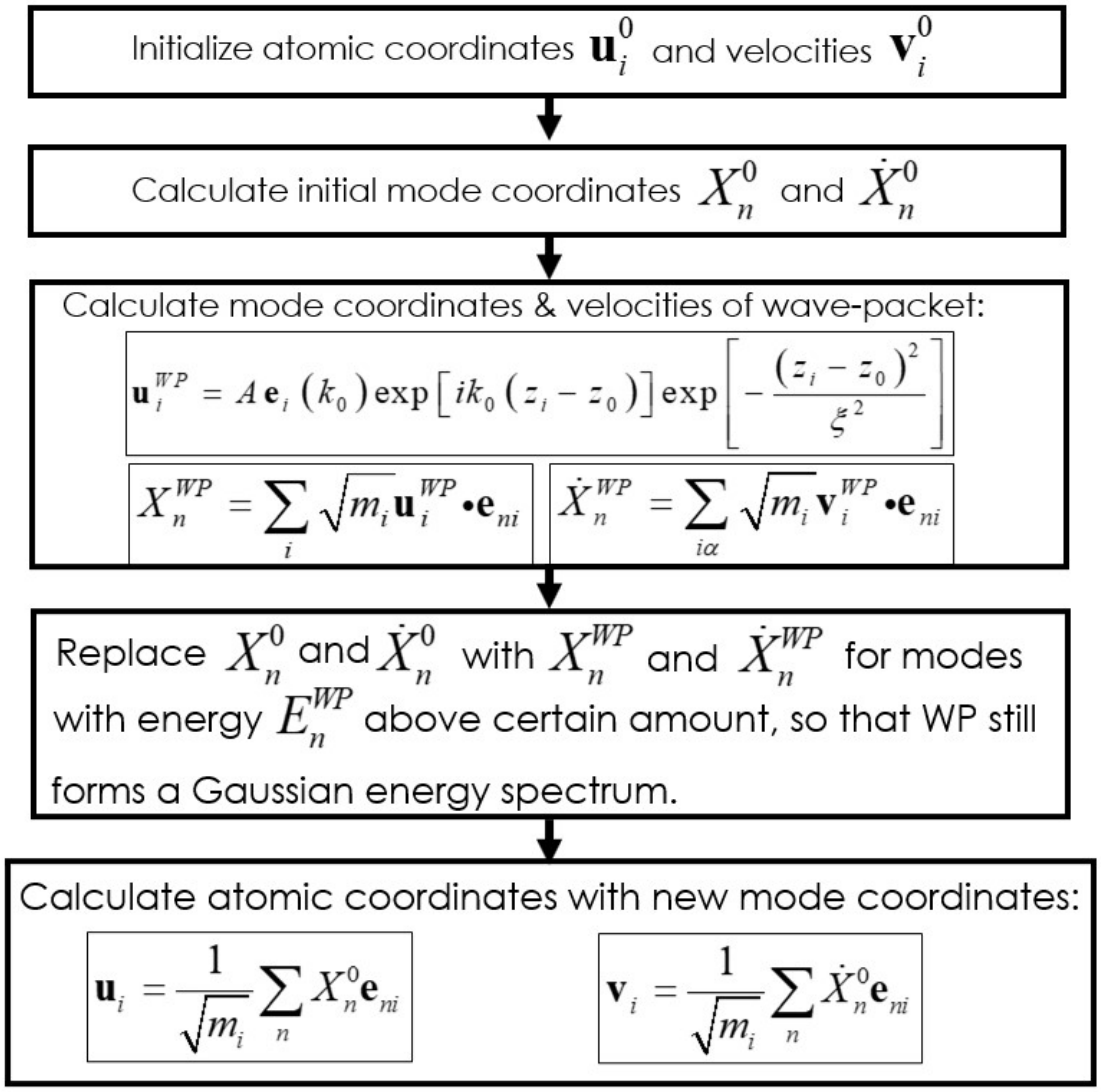

Figure 8. Procedure for creating wave-packets in a finite temperature environment.

As shown in Figure 8, we initialize atomic velocities as usual according to our desired temperature. This results in a certain distribution of mode velocities. Then we calculated mode coordinates associated with a wave-packet and replace coordinates of these wave-packet modes with the new coordinates. This results in a Gaussian shape when viewing the energy spectrum, where the center of the Gaussian is the frequency of the phonon wave-packet, as shown below.

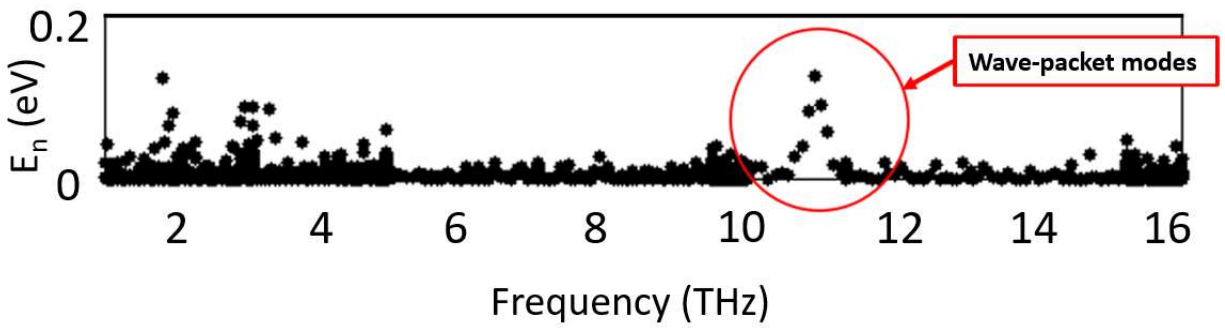

Figure 9. Energy spectrum of our 4320-atom silicon-germanium superlattice system, where black points show the energy of each mode. After readjusting the mode coordinates to form a Gaussian wave-packet at 10.9 THz, a Gaussian energy spectrum of the wave-packet is seen 10.9 THz.

To conclude, we define temperature in terms of atoms as usual, but readjust the mode coordinates to form a wave-packet afterwards. This has a small effect on the system temperature, for example by initializing the system with 300 K of energy, readjusting the mode coordinates to form a single wave-packet may change the total temperature by ~1%.

In the manuscript, we showed how the MCC3s compared to actual energy transfers of two wave-packets with reduced wave-vectors k=0.75 and k=0.99 in the [001] direction. The rest of the energy transfer results for the other wave-packets are shown here, noting the common trend of forming linear patterns. The energy transfer results for k=0.77 are shown below.

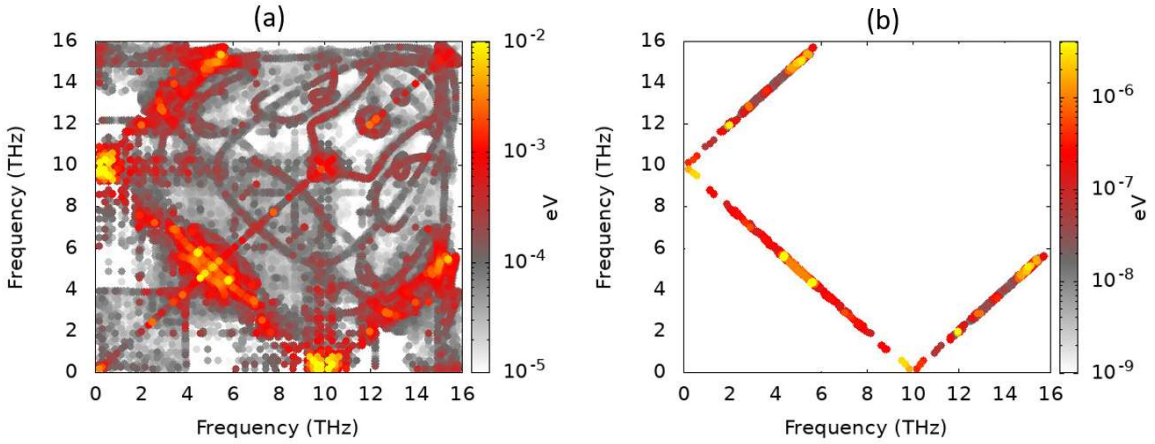

Figure 10. (a) Energy transfer pathways for the center mode of a k=0.77 LA wave-packet in the [001] direction, showing the linear patterns that form in the two-dimensional space of energy transfer pathways. (b) Components of the anharmonic phonon linewidths for the center k=0.77 LA wave-packet mode, calculated via the 2nd order perturbation theory expression for phonon linewidths.

Figure 10 shows the energy transfer pathways of a wave-packet with frequency 10 THz, showing that the scattering pathways tend to form linear patterns. This sort of behavior also arises in Fermi's golden rule via Equation 5, which predicts that the strongest components of the phonon scattering decay rate involve triplets of modes close together in frequency. For the Fermi's golden rule calculations in Figure 10 we used

$$\Gamma_n = \frac{\hbar\pi}{16\omega_n}\sum_{\mathbf{q}_1,\mathbf{q}_2}\sum_{ml}\left|\frac{K_{nml}}{\omega_m\omega_l}\right|^2$$
$$\times\Big[\left(f_1+f_2+1\right)\delta\left(\omega_n-\omega_1-\omega_2\right)$$
$$-\left(f_1+f_2+1\right)\delta\left(\omega_n+\omega_1+\omega_2\right)$$
$$+\left(f_1-f_2\right)\delta\left(\omega_n+\omega_1-\omega_2\right)$$
$$-\left(f_1-f_2\right)\delta\left(\omega_n-\omega_1+\omega_2\right)\Big]$$

which is the gamma point $\mathbf{q}=0$ form of Equation 5. This shows that the Fermi's golden rule expression for phonon decay rate at the gamma point is a decent descriptor of predicting dominant energy transfer pathways in a large supercell of atoms. More energy transfer pathways for the remaining wave-packet simulations are shown below.

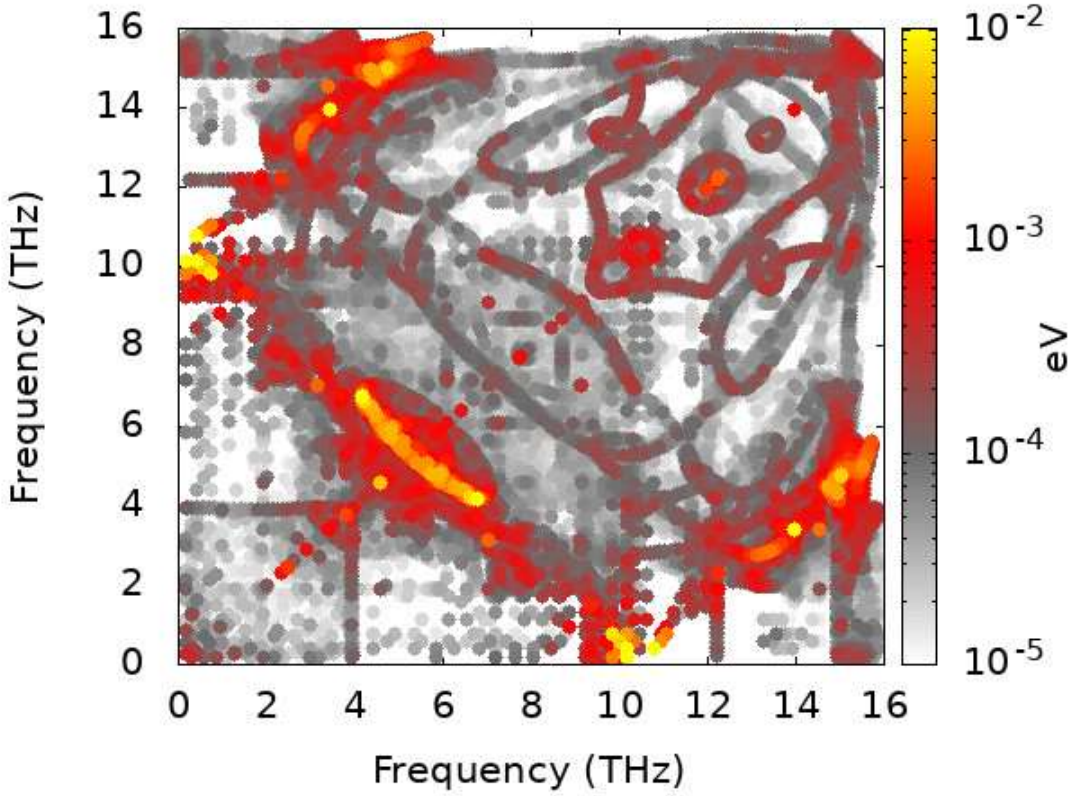

Figure 11. Energy transfer pathways for the center mode of a k=0.82 LA wave-packet in the [001] direction.

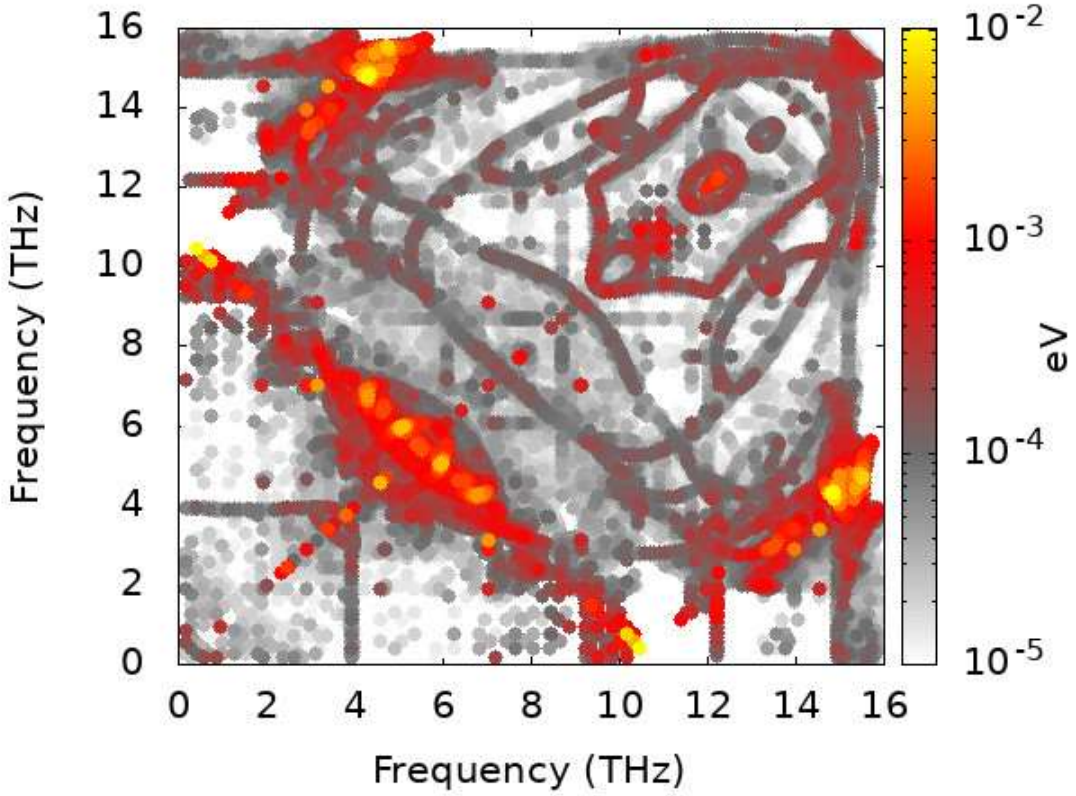

Figure 12. Energy transfer pathways for the center mode of a k=0.85 LA wave-packet in the [001] direction.

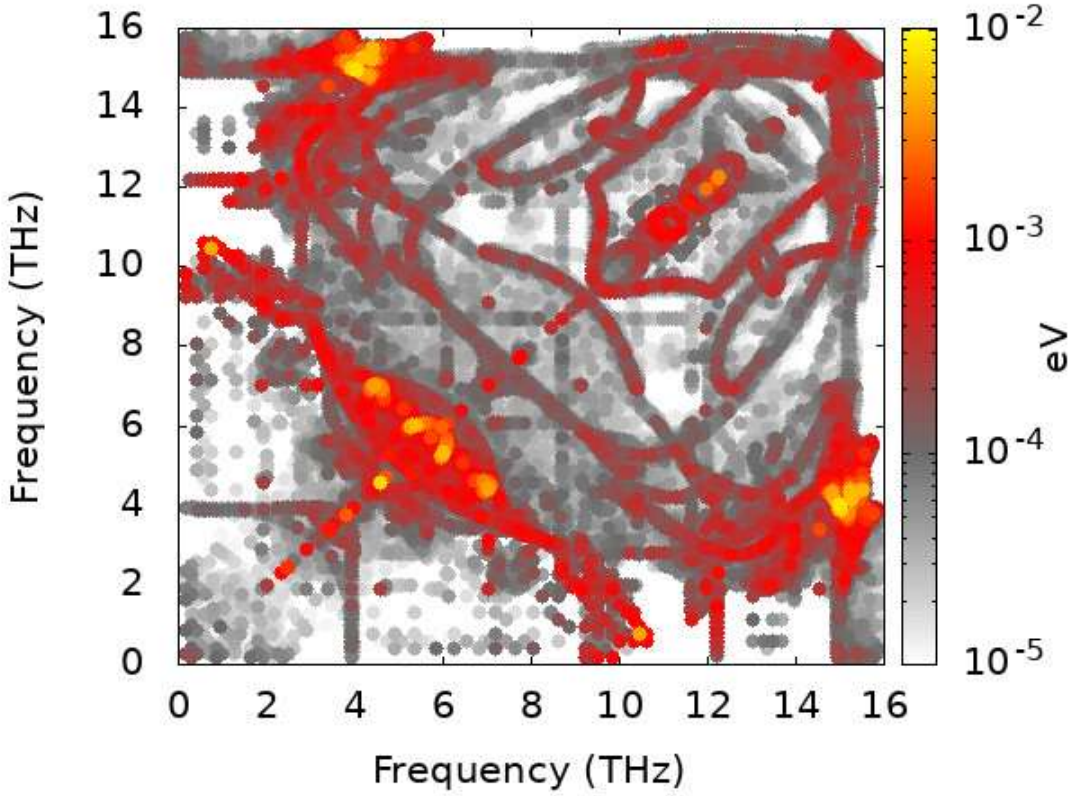

Figure 13. Energy transfer pathways for the center mode of a k=0.87 LA wave-packet in the [001] direction.

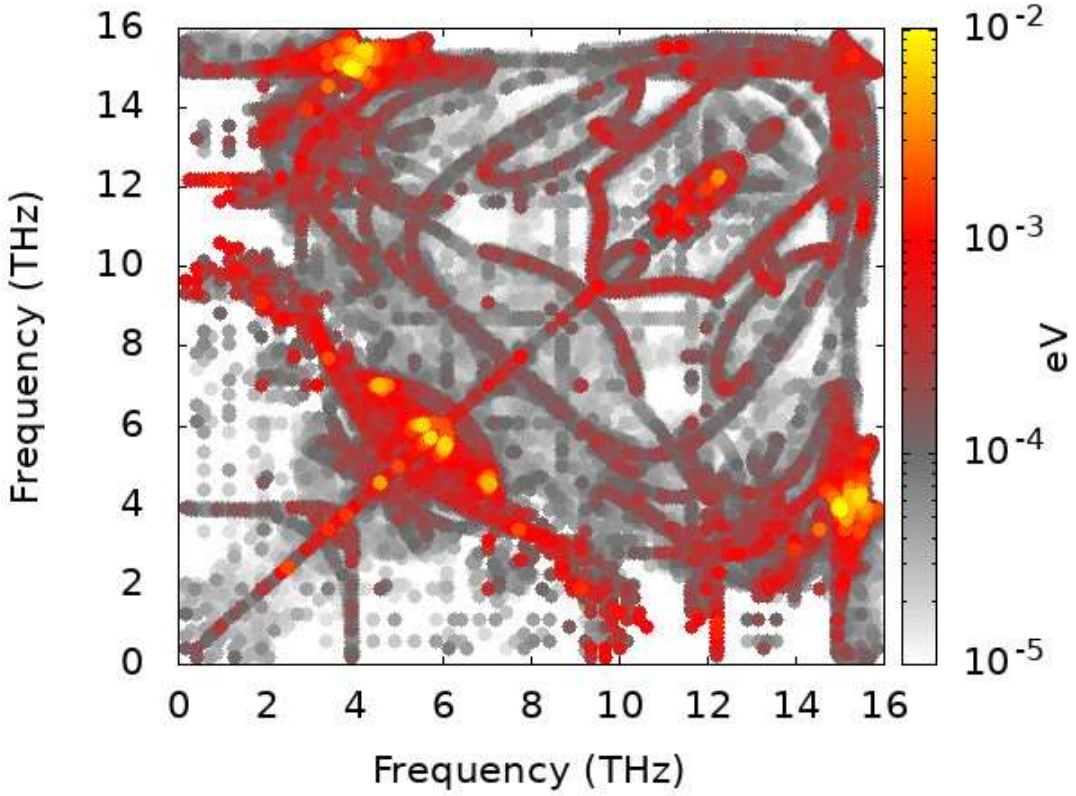

Figure 14. Energy transfer pathways for the center mode of a k=0.90 LA wave-packet in the [001] direction.

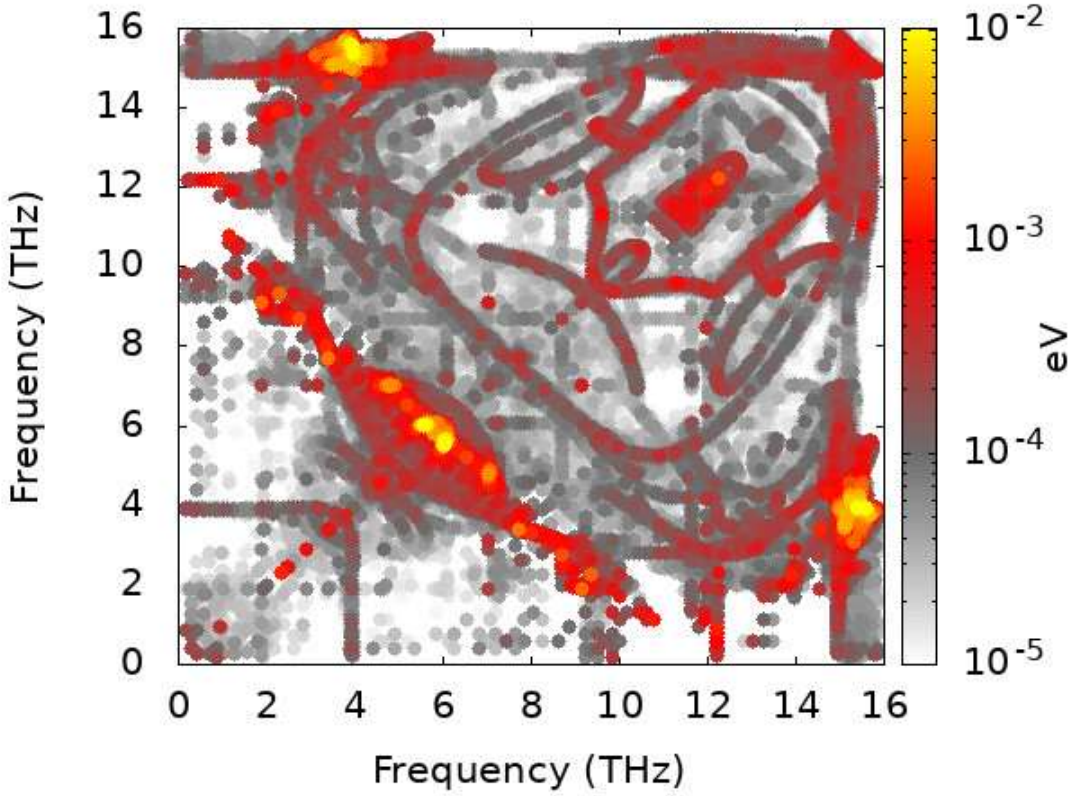

Figure 15. Energy transfer pathways for the center mode of a k=0.92 LA wave-packet in the [001] direction.

The common theme among all the energy transfer pathways for these wave-packet simulations is the existence of linear patterns, suggesting that the strongest mode energy transfer pathways involve triplets of certain frequencies, as also predicted by Fermi's golden rule for phonon decay rates in Equation 5. This provides more insight into Question 4 on how modes interact; clearly the top ~1% of coupling constants are most important, but there is also an important dynamical effect that causes mode triplets of certain frequencies to interact more strongly than others.

Interfacial heat transfer in mode coordinates.

In this manuscript we presented a formalism for modeling interactions and energy transfer between individual modes. Interactions between individual modes, however, does not explain how modes combine to transport heat across interfaces, because our mode energy transfer expressions only tell us which modes energy gets transferred to, instead of where that energy flows spatially (e.g. between two sides of an interface). To model interfacial heat flow we therefore seek to modify the mode power transfer expressions to include power transfer between two regions of space (i.e., two sides of an interface) instead of power transfer between individual modes.

To directly model how mode interactions contribute to interfacial heat transfer, we begin with the commonly used expression for power transfer $\dot{Q}^{AB}$ between two sides A and B of an interface[10,11]

$$\dot{Q}^{AB} = \sum_{i\in A}\sum_{j\in B} \mathbf{v}_i \bullet \frac{\partial H_j}{\partial \mathbf{u}_i} - \mathbf{v}_j \bullet \frac{\partial H_i}{\partial \mathbf{u}_j} \tag{10}$$

which is like force times velocity for each atom pair, where $\mathbf{v}_i$ and $\mathbf{u}_i$ are atomic velocity and displacement, respectively, and H_i is the Hamiltonian of atom i. In this expression, atoms i are include atoms of Side A while atoms j include atoms of Side B; this is therefore the net power transfer between sides A and B. We seek to get this expression entirely in terms of atomic displacements and velocities, so that we may convert to mode coordinates using $u_i^\alpha = \frac{1}{\sqrt{m_i}}\sum_n X_n e_{ni}^\alpha$ and $v_i^\alpha = \frac{1}{\sqrt{m_i}}\sum_n \dot{X}_n e_{ni}^\alpha$ where α is a Cartesian direction. We therefore use the Hamiltonian of a Taylor expansion potential so that $\frac{\partial H_j}{\partial u_i^\alpha} = \Phi_{ij}^{\alpha\beta} u_j^\beta + \frac{1}{2}\sum_{k\gamma} \Psi_{ijk}^{\alpha\beta\gamma} u_j^\beta u_k^\gamma$ and

$\frac{\partial H_i}{\partial u_j^\beta} = \Phi_{ij}^{\alpha\beta} u_i^\alpha + \frac{1}{2}\sum_{k\gamma} \Psi_{ijk}^{\alpha\beta\gamma} u_i^\alpha u_k^\gamma$. Substituting these into Equation 10, transforming the atomic displacements and velocities into mode coordinates, and rearranging the terms gives the mode interaction contributions to heat flow between two regions:

$$\dot{Q}^{AB} = \sum_{nm} K_{nm}^{AB} X_n \dot{X}_m + \sum_{nml} K_{nml}^{AB} X_n X_m \dot{X}_l + \cdots \tag{11}$$

where K_{nm}^{AB} are what we call the spatial mode coupling constants for 2nd order harmonic interactions (SMCC2s), K_{nml}^{AB} are the spatial mode coupling constants for 3rd order anharmonic interactions (SMCC3s), and so forth. The SMCC2s are given by

$$K_{nm}^{AB} = \sum_{i\in B}\sum_{j\in A}\sum_{\alpha\beta} \frac{\Phi_{ij}^{\alpha\beta}}{\sqrt{m_i m_j}} e_{mi}^\alpha e_{nj}^\beta - \sum_{i\in A}\sum_{j\in B}\sum_{\alpha\beta} \frac{\Phi_{ij}^{\alpha\beta}}{\sqrt{m_i m_j}} e_{ni}^\alpha e_{mj}^\beta \tag{12}$$

and the SMCC3s are given by

$$K_{nml}^{AB} = \sum_{i\in B}\sum_{j\in A}\sum_{k}\sum_{\alpha\beta\gamma} \frac{\Psi_{ijk}^{\alpha\beta\gamma}}{\sqrt{m_i m_j m_k}} e_{mi}^\alpha e_{nj}^\beta e_{kl}^\gamma - \sum_{i\in A}\sum_{j\in B}\sum_{\alpha\beta} \frac{\Psi_{ijk}^{\alpha\beta\gamma}}{\sqrt{m_i m_j m_k}} e_{ni}^\alpha e_{mj}^\beta e_{kl}^\gamma \tag{13}$$

where the difference between the left and right sums are which side (A or B) the atoms are summed over. The purpose of the two sums is that this is a net heat transfer, represented by transfer from A to B minus transfer from B to A. The utility of $\dot{Q}^{AB}$ written in the form of Equation 11 is that it shows why certain pairs of modes may transport heat more strongly than others, i.e. mode pairs with large spatial coupling constants should transport heat more effectively. The validity of this $\dot{Q}^{AB}$ expression is illustrated in Figure 16 below, where we perform an MD simulation of heat

flow from silicon (Side A) to germanium (Side B) in a Si-Ge superlattice, and compare the energy change of Side B with the time-integrated heat transfer $Q^{AB} = \int_0^t \dot{Q}^{AB} dt$.

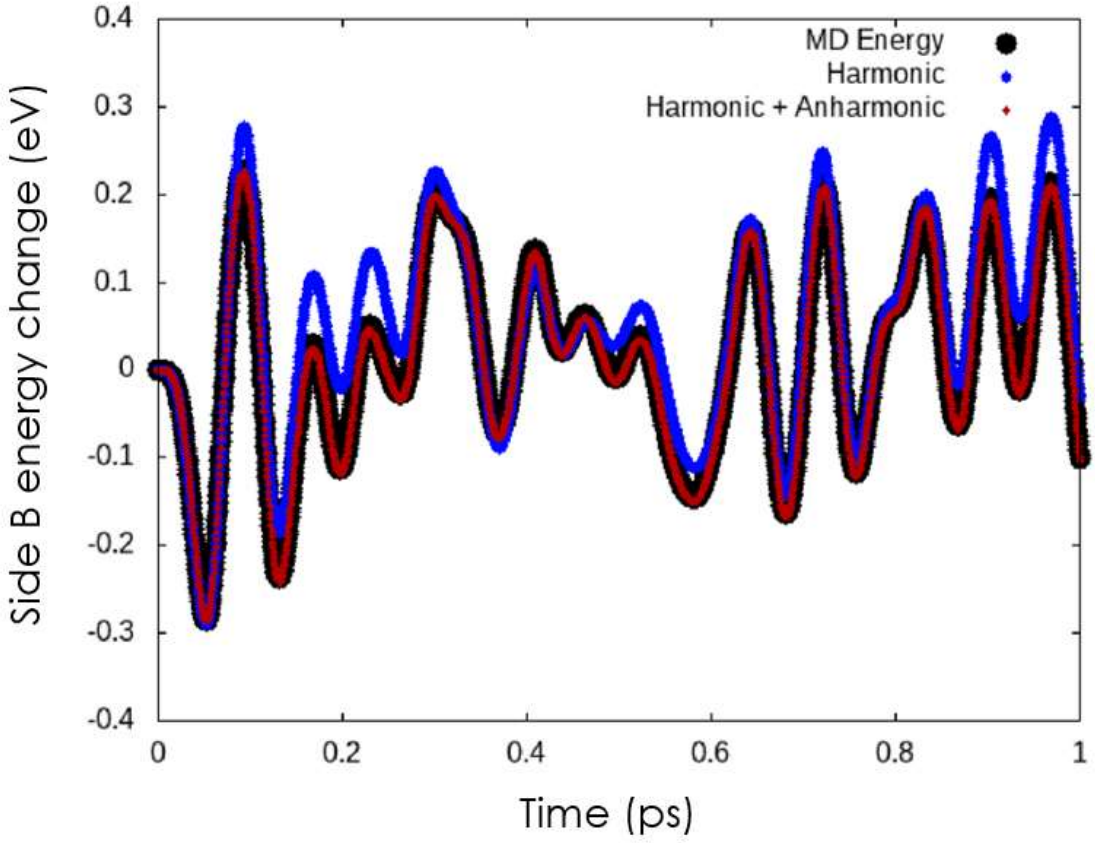

Figure 16. Simulation of heat flow from silicon (Side A) to germanium (Side B) to verify the mode interface heat flow expression of Equation 10. The black line is the total energy of all atoms in Side B. The red line is the time integral of the mode heat flow expression of Equation 11 including 2nd plus 3rd order terms. The blue line is the time integral of the mode heat flow expression of Equation 11 including 2nd order terms only.

To conclude, our formalism presented in the manuscript only describes how energy is transferred between individual modes, but not how these mode interactions result in energy

transport between two regions of space. To study interfacial heat transfer or interface conductance in terms of mode interactions, we need to use the $\dot{Q}^{AB}$ expression derived here. This will be the topic of a future paper.

References

1 Dove, M. T. & Dove, M. T. *Introduction to lattice dynamics*. (Cambridge university press, 1993).

2 Srivastava, G. P. *The physics of phonons*. (Routledge, 2019).

3 Rohskopf, A. <https://github.com/rohskopf/ModeCode> (2021).

4 Thompson, A. P. *et al.* LAMMPS-a flexible simulation tool for particle-based materials modeling at the atomic, meso, and continuum scales. *Computer Physics Communications* **271**, 108171 (2022).

5 Maradudin, A. & Fein, A. Scattering of neutrons by an anharmonic crystal. *Physical Review* **128**, 2589 (1962).

6 Tadano, T., Gohda, Y. & Tsuneyuki, S. Anharmonic force constants extracted from first-principles molecular dynamics: applications to heat transfer simulations. *Journal of Physics: Condensed Matter* **26**, 225402 (2014).

7 Shao, C., Rong, Q., Hu, M. & Bao, H. Probing phonon–surface interaction by wave-packet simulation: Effect of roughness and morphology. *Journal of Applied Physics* **122**, 155104 (2017).

8 Schelling, P., Phillpot, S. & Keblinski, P. Phonon wave-packet dynamics at semiconductor interfaces by molecular-dynamics simulation. *Applied Physics Letters* **80**, 2484-2486 (2002).

9 Cheng, Z. *et al.* Experimental Observation of Localized Interfacial Phonon Modes. *arXiv preprint arXiv:2105.14415* (2021).

10 Gordiz, K. & Henry, A. A formalism for calculating the modal contributions to thermal interface conductance. *New Journal of Physics* **17**, 103002 (2015).

11 Barrat, J.-L. & Chiaruttini, F. Kapitza resistance at the liquid—solid interface. *Molecular Physics* **101**, 1605-1610 (2003).